

Long-term effects of dam operations for water supply to irrigation on downstream river reaches. The case of the Ribb River, Ethiopia

Mulatu, Chalachew A.; Crosato, Alessandra; Langendoen, Eddy J.; Moges, Michael M.; McClain, Michael

DOI

[10.1080/15715124.2020.1750421](https://doi.org/10.1080/15715124.2020.1750421)

Publication date

2020

Document Version

Final published version

Published in

International Journal of River Basin Management

Citation (APA)

Mulatu, C. A., Crosato, A., Langendoen, E. J., Moges, M. M., & McClain, M. (2020). Long-term effects of dam operations for water supply to irrigation on downstream river reaches. The case of the Ribb River, Ethiopia. *International Journal of River Basin Management*, 19(4), 429-443.
<https://doi.org/10.1080/15715124.2020.1750421>

Important note

To cite this publication, please use the final published version (if applicable).
Please check the document version above.

Copyright

Other than for strictly personal use, it is not permitted to download, forward or distribute the text or part of it, without the consent of the author(s) and/or copyright holder(s), unless the work is under an open content license such as Creative Commons.

Takedown policy

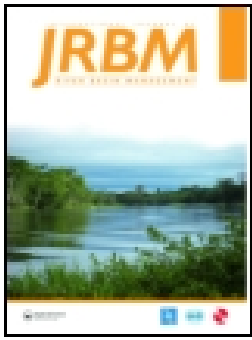
Please contact us and provide details if you believe this document breaches copyrights.
We will remove access to the work immediately and investigate your claim.

Green Open Access added to TU Delft Institutional Repository

'You share, we take care!' - Taverne project

<https://www.openaccess.nl/en/you-share-we-take-care>

Otherwise as indicated in the copyright section: the publisher is the copyright holder of this work and the author uses the Dutch legislation to make this work public.



Long-term effects of dam operations for water supply to irrigation on downstream river reaches. The case of the Ribb River, Ethiopia

Chalachew A. Mulatu, Alessandra Crosato, Eddy J. Langendoen, Michael M. Moges & Michael E. McClain

To cite this article: Chalachew A. Mulatu, Alessandra Crosato, Eddy J. Langendoen, Michael M. Moges & Michael E. McClain (2020): Long-term effects of dam operations for water supply to irrigation on downstream river reaches. The case of the Ribb River, Ethiopia, International Journal of River Basin Management, DOI: [10.1080/15715124.2020.1750421](https://doi.org/10.1080/15715124.2020.1750421)

To link to this article: <https://doi.org/10.1080/15715124.2020.1750421>



Published online: 26 Apr 2020.



Submit your article to this journal [↗](#)



Article views: 195



View related articles [↗](#)



View Crossmark data [↗](#)



Citing articles: 2 View citing articles [↗](#)



Long-term effects of dam operations for water supply to irrigation on downstream river reaches. The case of the Ribb River, Ethiopia

Chalachew A. Mulatu ^{a,b,c}, Alessandra Crosato ^{b,d}, Eddy J. Langendoen ^e, Michael M. Moges ^c and Michael E. McClain ^{a,b}

^aDepartment of Water Resources and Ecosystems, IHE Delft Institute for Water Education, Delft, The Netherlands; ^bFaculty of Civil Engineering and Geosciences, Delft University of Technology, Delft, The Netherlands; ^cFaculty of Civil and Water Resources Engineering, Bahir Dar Institute of Technology (BIT), Bahir Dar University, Bahir Dar, Ethiopia; ^dDepartment of Water Science Engineering, IHE Delft Institute for Water Education, Delft, The Netherlands; ^eDepartment of Agriculture, Watershed Physical Processes Research Unit, Agricultural Research Service, Washington, DC, USA

ABSTRACT

This work investigates the applicability of an analytical method for quick assessments of the long-term morphological effects of different dam operations on downstream river reaches with the idea to apply the method in feasibility studies to identify the least morphologic-impacting operation scenario. The Ribb River (Ethiopia) is used as a study case. The analytical method estimates the idealized, new equilibrium of the river bed profile without considering the duration of the morphological evolution. We apply the analytical method distinguishing sand-bed from gravel-bed reaches. The outcome of the analytical method is compared to that of a calibrated one-dimensional river morphology computer model. The analytical method overestimated the morphological changes compared to the one-dimensional model. By establishing the upper limits of the impact, the analytical method identifies a theoretical maximum river bed degradation near the base of the dam. If all sediment is trapped in the reservoir, the method allows distinguishing the effects of different dam operation scenarios, but only for gravel-bed river reaches. However, the method can also be applicable for sand-bed reaches if there is sediment input from the upper reaches. Further research works should be done to validate both methods if they indeed allow to detect the least impacting scenario, considering that data showing the effects of long-term dam operations on the downstream river reaches are lacking.

ARTICLE HISTORY

Received 14 September 2019
Accepted 29 March 2020

KEYWORDS

Dam operation scenario; equilibrium Theory; morphological time scale; Ribb River; SOBEK-RE

1. Introduction

Dams are vital for the economic development of regions due to the need of storing water for different activities, such as power generation and irrigation. However, dams have major impacts on downstream river reaches. They change the discharge regime; in particular, the timing, duration, and magnitude of low and high flows (Grant, 2012; Williams & Wolman, 1984). In addition, dams also change the sediment regime, since they trap almost all the incoming bed load and a portion of the suspended load; the reservoir's trapping efficiency depends, among others, on the size and shape of the reservoir and its operation (Basson, 2004; Brune, 1953; Kondolf et al., 2014a, 2014b). In response to the changes in discharge and sediment regimes, the channel downstream of the dam adjusts its morphology by altering its planform, slope, width, depth, and sediment characteristics through time.

Both channel bed degradation and aggradation are the primary channel responses have been observed downstream of dams (Schmidt & Wilcock, 2008; Williams & Wolman, 1984). For example, up to 7.5 m of river bed lowering has been observed downstream of the Hoover Dam on the Colorado River, USA; degradation extended to 21 km downstream 6 months after dam closure, 28 km after 1 year, 50 km after 2 years and over 120 km after 5 years (Williams & Wolman, 1984). Degradation may eventually change the river planform, from braided to meandering (Kondolf, 1997). River bed material coarsening and armour layer formation may

continue until the released flow is unable to entrain the bed material (Holly & Karim, 1986; Kondolf, 1997; Williams & Wolman, 1984). On the other hand, if the regulated flows are not able to move sediments supplied by tributaries, the river bed may aggrade (Williams & Wolman, 1984). Long term operation of dams may also change the concavity of the downstream river bed profile and result in bed material fining (Michael Nones et al., 2019; Varrani et al., 2019). Channel widening, bar formation, braiding, increased sinuosity (Shields et al., 2000) and reduced channel conveyance capacity (Sanyal, 2017) are further frequent consequences. Generally, the overall morphological impacts of dam construction depend on the river size and reservoir capacity, pre- and post-dam hydrologic regimes, environmental setting, initial channel morphology and dam operation (Church, 1995; Graf, 2006; S Li et al., 2018; Petts & Gurnell, 2005; Schmidt & Wilcock, 2008; Williams & Wolman, 1984; Yang et al., 2011).

A generalized prediction of dam-induced impacts on downstream channel morphology is difficult, as the drivers and processes are site-specific and complex interactions exist among these drivers (Graf, 2006). A number of assessment methods have been developed with varying complexity. Williams and Wolman (1984) performed an empirical analysis using data of different river systems. Petts (1979), Brandt (2000) and Petts and Gurnell (2005) developed conceptual models. Grant et al. (2003), Curtis et al. (2010) and Schmidt and Wilcock (2008) developed channel response

predictive models for general applications. In addition, numerous one-dimensional (1D), two-dimensional (2D) and three-dimensional (3D) morphodynamic codes are available to analyse dam-induced morphologic changes (Khan et al., 2014; Omer et al., 2015). 1D models have advantages for large-scale studies, as they are less data intensive and computationally efficient while providing an acceptable general representation of the river system (Berends et al., 2015). These models are appropriate to study the dam-induced effects at the preliminary and feasibility stages of dam design and to optimize dam operation scenarios (M Nones et al., 2014; Van der Zwet, 2012). They also allow to analyse the time evolution of river morphology, and can establish the duration to reach a new equilibrium, as well as the temporal evolution of local river characteristics like sediment transport rates, water level changes and river bed elevation.

The long-term morphological effects of different dam operations on downstream river reaches can also be assessed using simple, easy to apply, analytical methods, for example the Equilibrium Theory (ET) developed by Jansen et al. (1979). Such analytical methods have the following advantages compared to 1D (and greater) computer models: much fewer data are required; reduced setup, calibrate, and run time; and therefore reduced costs. The ET method estimates the theoretical river bed slope, which would be attained a long time after impoundment, caused by the changed discharge and sediment transport regimes. This method, however, is unable to predict the time required to reach the final equilibrium state and the transition phases of the morphological development.

In the absence of river reaches with historical pre-dam and post-dam bed profile data, it is impossible to assess how well the above-mentioned methods assess the morphological changes. Additionally, if historical data related to the pre-dam period are lacking in systems that have been impounded in the past, it is unknown if the downstream reaches have attained a condition close to a new equilibrium. These limitations are especially true for rivers in Africa, like those of the Upper Blue Nile basin, Ethiopia, where most dams have been constructed during last decades (Koga dam), or are planned (Gilgel Abay and Gumara dams) or are under construction (Ribb and Megech dams). Determining the least morphologically impactful dam operation scenario is the critical to the regional use of water resources.

The overall goal of the presented study is to establish whether the ET method allows identifying the least-impactful dam operation scenario so it can be used in the preliminary dam design phases. The Ribb River located in the Upper Blue Nile basin, Ethiopia, is our case-study. A dam for irrigation purposes is under construction 77 km upstream of the river mouth. Downstream of the dam the river includes gravel- and sand-bed reaches for which hydrologic and geomorphic data are available (Mulatu et al., 2018). To assess the applicability of the ET method, its results are compared to those from a calibrated 1D morphodynamic model developed using the SOBEK-RE software. The software has been applied for similar purposes by Van der Zwet (2012) for the White Volta River, Ghana, to analysis the morphological change due to damming and found river bed degradation just downstream of the dam and propagates in downstream direction through time of dam operation for the alluvial deposit river reach.

2. Study case: the Ribb River

The Ribb River originates in the Guna Mountains (Lake Tana sub-basin, Figure 1(a)), where the elevation reaches 4,000 m a.s.l. and drains to Lake Tana at an elevation of 1,787 m a.s.l, the source of the Blue Nile River. Its basin encompasses an area of 1,865 km² (Figure 1(b)). The climatic condition of the basin is tropical highland monsoon (Setegn et al., 2008) with a yearly average rainfall of 1,300 mm (Debre Tabor Metrological station of the years 1988–2015); 80% of it occurring between June and September.

A 73 m high dam (called ‘Ribb Dam’) and a diversion weir, located 32 km downstream of the dam, are under construction to irrigate 15,000 ha of farmland (BRLi and MCE, 2010). The reservoir will have a capacity to impound 234 million m³ of water and inundate 10 km² of surface area at the Normal Pool Level (NPL) elevation of 1,940 m a.s.l. The released irrigation demand and the environmental flows will flow through the river channel until diverted by the weir to the irrigated lands. Hence, after the start of dam operation, the river reach between dam and weir will carry a dry time discharge of 16.4 m³ s⁻¹ or larger. The river reach downstream of the diversion weir will only receive an environmental flow of 0.17 m³ s⁻¹ or less during the dry period and the regulated flow during rainy season.

The study river reach has two gauging stations (Figure 1(b) and (c)). The upper station is located 3.5 km downstream of the dam. This location has an average daily discharge of 8.3 m³ s⁻¹ and encompasses a watershed area of 844 km². The lower station is located near the Ribb Bridge that connects the cities of Bahir Dar and Gondar. This location has an average daily discharge of 15 m³ s⁻¹ and encompasses a watershed area of 1,592 km².

Mulatu et al. (2018) divided the river downstream of the dam into four reaches (the Upper-I, the Upper-II, the Middle and the Lower) based on the presence of natural and man-made river bed fixations (rock outcrops, diversion weir, and bridge) (Figure 1(c)). The reaches differ according to their bed material, average river bed slope, and channel width, as well as anthropogenic interventions (embankment construction, water abstraction and, sand mining). Planimetric, geometric and granulometric characteristics of the study reaches were analyzed by Mulatu et al. (2018). The main parameters needed for this study are summarized in Table 1.

3. Material and methods

We applied a physics-based analytical method derived from the ET, developed by Jansen et al. (1979), and a 1D model constructed using the SOBEK-RE software (<http://sobek-re.deltares.nl/index.php>) to estimate the expected long-term morphological changes of the Ribb River downstream of the Ribb Dam. Several dam operation scenarios were considered. The results of the two applications were then compared to assess the applicability of the ET for the preliminary dam designs. The Ribb River has distinct sand-bed (Lower and Middle) and gravel-bed (Upper-I and Upper-II) reaches; the latter may present a limit to bed degradation due to bed armouring. The detailed description of the methods, the required input data and the boundary conditions for the ET and the 1D model are presented in the next sections.

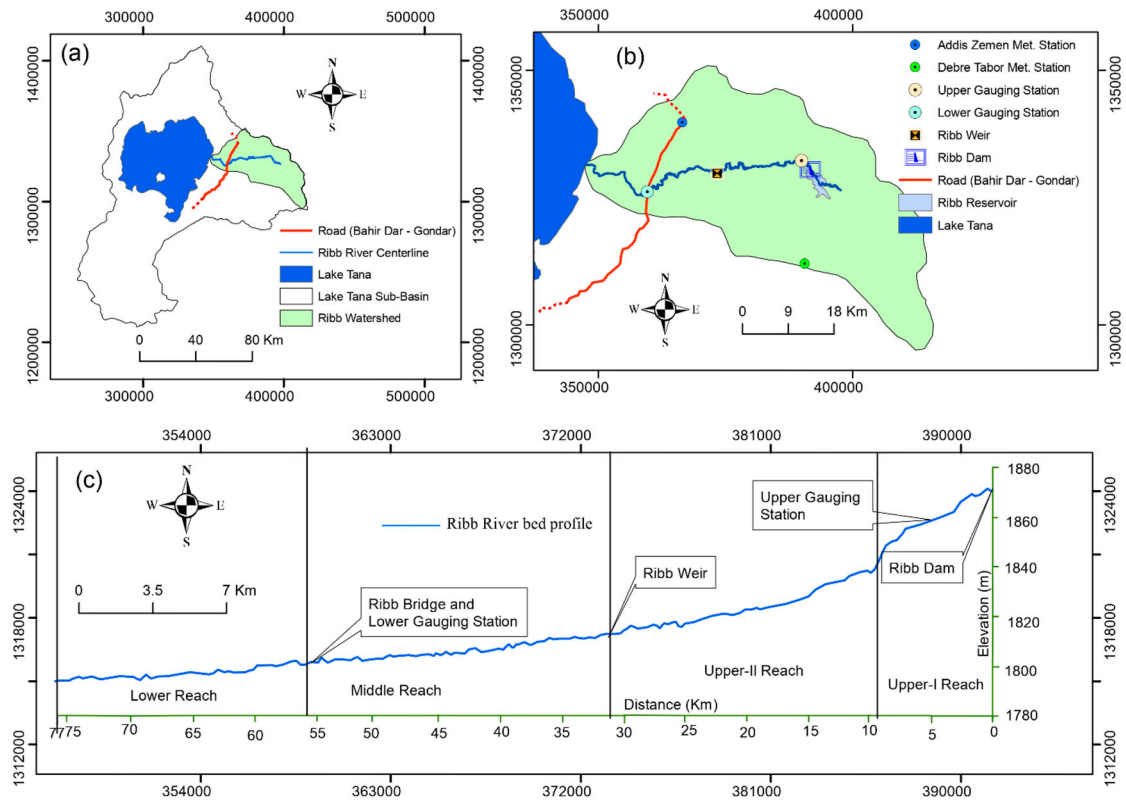


Figure 1. Geographical setting of the Ribb River. (A) Lake Tana sub-basin showing Ribb River watershed and its main stream, (B) location of measurement stations, dam and weir in the Ribb River watershed, and (C) river bed profile and sub-division into reaches.

Table 1. Reach-average characteristics of the Ribb River below the Ribb Dam.

Reach	Reach length (km)	Reach-averaged bankfull width (m)	Reach-averaged bankfull depth (m)	Reach-averaged channel bed slope (%)	Median grain size (D_{50}) (mm)	Mean grain size D_m (mm)	D_{90} (mm)
Upper-I	10	65	4.3	0.30	7.0	9.7	12
Upper-II	22	58	4.8	0.12	7.0	7.5	11
Middle	25	46	5.2	0.04	0.65	3.0	5.5
Lower	20	38	5.5	0.037	0.35	0.5	0.6

3.1. Data sources

The required data for the study were collected from the literature and provided by Ethiopian agencies. For instance, the current reach-averaged river bed slopes, cross-sections and the reach-averaged river bed-materials characteristics were derived from Mulatu et al. (2018), who collected required data and bed-material samples to analyse the current morphodynamic trends of the Ribb River, i.e. before dam construction. The daily time series discharge at the Lower and Upper gauging stations and the water levels at the Lower gauging station covered the period 1995–2010, and were collected by the Ministry of Water, Irrigation and Energy of Ethiopia (MoWIE). The discharge data were used to compute the reach-averaged pre-dam sediment transport capacity and for water balance analysis, while the water levels were used for the calibration and validation of the 1D model. The monthly average rainfall and evaporation at the reservoir surface of the same period were obtained from the Ribb Dam feasibility study and design documents (Figure 2). These documents, provided by the MoWIE, were also used as a data source to develop realistic dam operation scenarios.

3.2. Dam operation scenarios

The reservoir operation was designed to irrigate 15,000 ha of command area for the specified monthly irrigation water

requirement and environmental releases (WWDSE and TAHAL, 2007), Figure 2. However, the dam may be operated in the future for a larger or smaller command area, deviating from the design. For example, the Ribb Dam Feasibility Study document (WWDSE and TAHAL, 2007) suggests that the stored water may be released to irrigate 19,925 ha of command area, which is 32.8% greater than the design.

Taking this into account, we considered three scenarios: Scenario-I (Sc-I) corresponding to a command area of 13,500 ha (10% smaller from the design); Scenario-II (Sc-II) corresponding to a command area of 15,000 ha (equal to the design); and Scenario-III (Sc-III) corresponding to a command area of 19,925 ha (32.8% greater from the design). Dam releases to irrigate the proposed command areas (irrigation water requirements) for each scenario were provided as monthly discharges (Table 2). However, the actual water release may not correspond to either of the studied scenarios, as it will depend on the actual cropping pattern and the amount of rainfall in the area. In all dam operation scenarios, the dry month discharge downstream of the weir will constitute the ecological flow, which is $0.17 \text{ m}^3 \text{ s}^{-1}$ or lower (BRLI and MCE, 2010).

Once the reservoir is full, the wet season excess volume of water above the NPL elevation will be released by the spillway. The spill-over discharge is here determined by applying a reservoir water balance based on the continuity equation

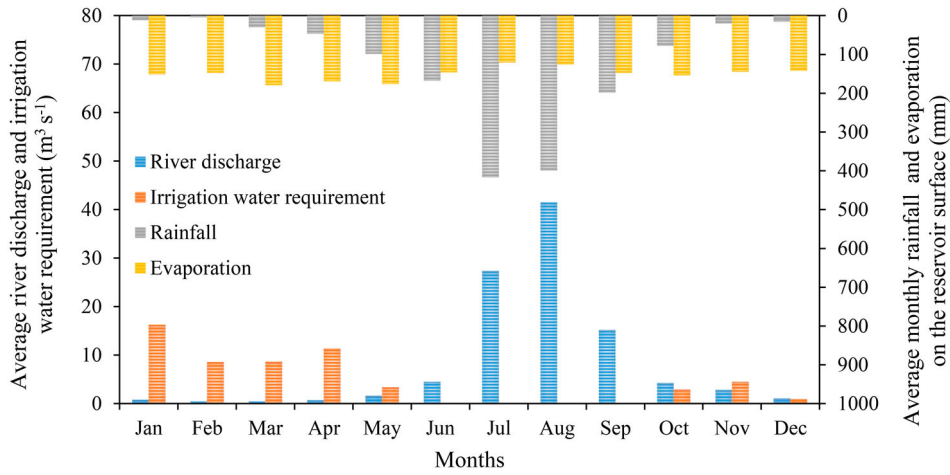


Figure 2. Comparison of average monthly river discharge at the Upper gauging station ($\text{m}^3 \text{s}^{-1}$), irrigation water requirement ($\text{m}^3 \text{s}^{-1}$), monthly average rainfall over the reservoir (mm) and monthly average estimated evaporation at the reservoir surface (mm). Data source: Study document for the feasibility of Ribb Dam (WWDSE and TAHAL, 2007).

Table 2. Monthly crop water requirements for the dam operation scenarios.

Scenario	Monthly crop water requirements ($\text{m}^3 \text{s}^{-1}$)								
	Jan	Feb	Mar	Apr	May	Jun to Sep	Oct	Nov	Dec
Sc-I	14.62	7.7	7.81	10.26	3.02	0	2.67	4.06	0.86
Sc-II	16.24	8.56	8.68	11.4	3.36	0	2.97	4.51	0.95
Sc-III	21.57	11.37	11.53	15.14	4.46	0	3.94	6.00	1.26

(Equation 1).

$$\text{Reservoir volume change} = \text{Average inflow} - \text{Average outflow} \quad (1)$$

The river discharge and rainfall over the reservoir are considered as inflow, whereas seepage, evaporation, environmental flow, and irrigation water requirements are considered as outflow. WWDSE and TAHAL (2007) estimated the seepage loss to be 25% of the monthly environmental flow.

The volume of rainfall and evaporation over the reservoir are surface-area dependent and hence, an Elevation – Area – Volume relationship of the reservoir was developed from the available topographic data of the reservoir area. For simplicity, a monthly time step was considered, even though this will reduce the outflow peaks and affect the results of yearly sediment transport capacity. The reservoir volume loss due to sediment accumulation through time was not considered for the water balance analysis. WWDSE and TAHAL (2007) estimated a reservoir storage loss of 0.22% per year. As sediment supply to the reservoir is dynamic and mainly depends on land use and land cover, population density, climate change, etc., there exists significant uncertainty in the expected storage loss and therefore its possible impact on our water balance analysis. Though note, reservoir sediment accumulation will reduce the reservoir volume over time and increase the spill-over discharge events, which will result in increased downstream morphological activity.

The pre-dam discharges were derived using the time-series discharge data at the Upper and the Lower gauging stations. The irrigation water requirements, the environmental releases, the lateral inflow, and the spill-over discharge were used to derive the post-dam downstream discharge characteristics.

3.3. Sediment transport capacity

As described by Mulatu et al. (2018), the Upper-I and the Upper-II reaches of the river system are dominated by gravel, while the Middle and the Lower reaches by sand. The Meyer-Peter and Müller (1948) sediment transport formula (Equation 2) revised by Wong and Parker (2006), assuming no bedforms ($\mu = 1$), and the Engelund and Hansen (1967) sediment transport formula (Equation 3) were selected to compute the sediment transport capacity of the gravel and sand dominated river reaches, respectively. These equations were selected as they are developed for gravel and sand dominated systems, respectively.

$$Q_s = \frac{4B\sqrt{g}}{\Delta} (hi - 0.047\Delta D_m)^{\frac{3}{2}} \quad (2)$$

$$Q_s = \frac{Bu^5}{20C^2\Delta^2 D_{50}\sqrt{g}} \quad (3)$$

in which Q_s is the volumetric sediment transport rate without pores ($\text{m}^3 \text{s}^{-1}$), B and h are the reach-averaged channel width and flow depth (m), respectively, i is the water surface slope (-), u is the flow velocity (m s^{-1}), C is the Chézy coefficient ($\text{m}^{1/2} \text{s}^{-1}$), Δ is the submerged specific gravity of sediment (1.65), D_{50} is the median grain size (m), D_m is the arithmetic mean grain size (m) given by $D_m = \sum p_i D_i$, p_i is the probability of the size fraction with diameter D_i (m) and g is acceleration due to gravity (9.81 m s^{-2}).

The Lower reach can have significant overbank flow during the rainy season (Mulatu et al., 2018; SMEC, 2008). Therefore, the measured discharge at the Lower gauging station is not representative for the entire reach. Hence, the computation of the reach-averaged sediment transport capacity for this reach may have some uncertainty. For this reason, the Lower reach is excluded from the analytical model application.

The pre-dam reach-averaged sediment transport capacity of the river was estimated by Mulatu et al. (2018) using daily river discharges. Here, however, as the post-dam outflow discharge was given on a monthly basis, we computed the pre-dam sediment transport using a monthly average discharge. In this way the annual sediment transport rate of the Ribb River might be underestimated, but this is still acceptable considering that the results are used to compare scenarios, all based on monthly discharges.

3.4. Reach-scale morphodynamic equilibrium theory

A river reach can be considered in morphodynamic equilibrium if the on-going reach-scale morphological changes can be considered negligible. This is true only if the volume of sediment entering the river reach equals the volume of sediment leaving the same river reach during a chosen time interval. Any new interventions on a river reach in morphodynamic equilibrium trigger a new trend of erosion and deposition, which ultimately leads to a new reach-scale equilibrium characterized by different values of the morphological variables, such as reach-averaged longitudinal slope, channel width, sediment size and bed roughness. This means that the river adapts its longitudinal bed slope and the other reach-averaged characteristics to the new external forcing, and this adaptation occurs during a transition period which can be rather long (tens to hundreds of years), depending on sediment transport rate and size of the river channel.

The Equilibrium Theory was developed by Jansen et al. (1979). The theory compares two reach-scale morphodynamic equilibrium conditions: one before (old equilibrium condition) and the other one a long time after a change of forcing has occurred (new equilibrium condition). The old and new equilibrium states are characterized by their longitudinal bed slope, channel width, water discharge and sediment transport regimes. The method was used here to estimate the theoretical river bed slope attained a long time after impoundment due to the changed discharge and sediment transport regimes. The theory has been recently extended by, for instance, (i) W Li et al. (2014) to predict the equilibrium bed profiles and water discharge for water diversions, (ii) Blom et al. (2017) to determine the equilibrium channel geometry of the alluvial river for variable flow relating with the channel width, bed material texture and channel slope, (iii) Bolla Pittaluga et al. (2014) to investigate the reach-scale quasi-equilibrium bed profile by applying a 1D morphodynamic model, and (iv) Lanzoni et al. (2015) to develop a 1D morphodynamic model to estimate the formative discharge that caused the observed (current) river bed slope of the Po River, Italy.

The methodology is developed based on the following major assumptions: (i) the river is fully alluvial, (ii) the river flow is uniform with a given width and a large width to depth ratio, (iii) the Chézy coefficient, the sediment composition and the degree of non-linearity of the sediment transport formula remain unchanged, and (iv) the river morphological response is based on the derivation of longitudinal slope and representative water depth.

The methodology was developed by combining the following equations:

- (1) Continuity equation of water.

$$Q_w = Bhu \quad (4)$$

- (2) Momentum equation for water, reduced to Chézy's equation for steady uniform flow and for large flow width-to-depth ratios.

$$u = C\sqrt{hi} \quad (5)$$

- (3) Simplified sediment transport capacity formula expressed as a power law of flow velocity.

$$q_s = a(u - u_c)^b \quad (6)$$

- (4) Sediment balance equation.

$$Q_s = q_s B \quad (7)$$

where Q_w is the flow discharge ($\text{m}^3 \text{s}^{-1}$), u_c is the critical flow velocity for initiation of sediment particle motion (m s^{-1}), a is the sediment transport proportionality coefficient (-), q_s is the volume of transported bed sediment (without pores) per unit of channel width ($\text{m}^2 \text{s}^{-1}$), and b is the degree of non-linearity of the sediment transport formula assumed to be 5 when using the Engelund and Hansen sediment transport formula.

3.4.1. Equilibrium bed slope for gravel-dominated river reaches

For the gravel-bed reaches, the average yearly sediment transport capacity of the river is computed using Equation (2), based on monthly discharges. Sediment is transported by the water only if the flow velocity exceeds the critical value for particle motion.

According to the characterization of dams by the International Commission on Large Dams (ICOLD, 1998), the Ribb Dam will store all of the incoming bed loads and the majority of suspended loads. This means that the future sediment input to the downstream reaches can be considered negligible. Post-dam released discharge values, for which the corresponding flow velocity exceeds the limiting value for sediment entrainment (u_c), will have the capacity to entrain sediment from the river bed and transport it downstream. Upstream bed erosion results in decreasing bed slope. The process continues until the final equilibrium bed slope that yields zero sediment transport is attained. At this point, the river bed material becomes immobile for all discharges, and in particular for the largest dam released discharge. Hence, the maximum dam released monthly discharge was used here to estimate the final river bed slope which will be attained after long years of dam operation. This is the slope for which the sediment transported by the highest discharge has become zero (achievement of critical conditions). The post-dam water depth at the largest released discharge ($h_{M\infty}$) and zero sediment transport can be obtained from Equation (2) combined with Equations (4) and (5) assuming the bed roughness, channel width and sediment size remain unchanged.

$$h_{M\infty} = \frac{Q_{wM}}{BC\sqrt{(0.047\Delta D_m)}} \quad (8)$$

in which Q_{wM} is the highest monthly discharge released by the dam ($\text{m}^3 \text{s}^{-1}$).

The final river bed slope (i_∞) which yields zero sediment transport is obtained from Equation (2), and is written as:

$$i_\infty = \frac{0.047\Delta D_m}{h_M \infty} \quad (9)$$

Assuming constant Chézy coefficient and grain size is a limitation of the approach as they might both increase after the start of dam operation (Grant, 2012; Williams & Wolman, 1984). However, as described by Di Silvio and Nones (2014), morphodynamic results obtained by using uniform bed materials are sufficiently significant for the analysis of future morphodynamic response.

3.4.2. Equilibrium bed slope for sand dominated river reaches

The total yearly sediment transport capacity for the sand-bed Middle river reach was derived using the Engelund and Hansen (1967) sediment transport formula, Equation (3). Combining the continuity and momentum equations for water and the sediment transport and sediment balance equations, the slope before and after dam operation for variable discharge (here monthly average) are given in Equations (10) and (11), respectively. These equations are derived considering the monthly discharge of the river with the same probability density of 1/12, in which k represents the specific month.

$$i_0 = \frac{Q_{s0}^{3/b_0} B^{(1-3/b_0)}}{a_0^{3/b_0} C_0^2} \left(\frac{1}{\sum_{i=1}^k \frac{1}{k} Q_{w0k}^{b_0/3}} \right)^{\frac{3}{b_0}} \quad (10)$$

$$i_\infty = \frac{Q_{s\infty}^{3/b_\infty} B^{(1-3/b_\infty)}}{a_\infty^{3/b_\infty} C_\infty^2} \left(\frac{1}{\sum_{i=1}^k \frac{1}{k} Q_{w\infty k}^{b_\infty/3}} \right)^{\frac{3}{b_\infty}} \quad (11)$$

In Equations (10) and (11), the subscripts '0' and '∞' indicate the values at the initial (just before dam operation) and final (a long time after dam operation) equilibrium states, respectively.

The ratio between river bed slope at the final and at the initial equilibrium states for variable discharge, assuming constant sediment transport exponent, b , sediment transport proportionality coefficient, a , river width, B , and Chézy coefficient, C , is given by Equation (12). This equation was used to compute the final equilibrium state of the river bed slope for the Middle river reach.

$$\frac{i_\infty}{i_0} = \left(\frac{Q_{s\infty}}{Q_{s0}} \right)^{\frac{3}{b}} \left(\frac{\sum_{i=1}^k Q_{w0k}^{b/3}}{\sum_{i=1}^k Q_{w\infty k}^{b/3}} \right)^{\frac{3}{b}} \quad (12)$$

3.4.3. Application to the Ribb River

The application of the analytical method allows us to assess the theoretical long-term response of the Ribb River due to altered discharge and sediment transport regimes caused by prolonged dam operation. The river reaches are assumed in a state of morphodynamic equilibrium at the moment of the intervention (i.e. no sediment accumulation or losses). This might not be true for the Ribb River, as there is a reduction in sediment transport capacity in the downstream

direction along the reaches, leading to progressive aggradation and channel blockage starting 4 km downstream of the Ribb Bridge (Mulatu et al., 2018).

3.5. Morphodynamic model application

3.5.1. Model description

SOBEK-RE is a 1D modelling tool for open channel networks computing water flow, sediment transport (uniform and graded sediment) and morphological changes for compound river channels, considering main channel and floodplains separately (<http://sobek-re.deltares.nl/index.php/documentation>). The model comprises three modules: (i) the water flow module, described by the continuity (Equation 13) and momentum (Equation 14) equations for water; (ii) the sediment transport module, which allows selecting among five standard sediment transport capacity formulas plus a user-defined one; and (iii) the morphological module, describing the bed level adaptation through time (Equation 15) based on the sediment balance equation (Exner, 1925). To prevent any differences between the ET method and 1D model to be caused by the selected sediment transport equations, the sediment transport formulae of Meyer-Peter and Müller (1948), revised by Wong and Parker (2006), and Engelund and Hansen (1967) were also used in the SOBEK-RE to compute the sediment transport capacity for the gravel and sand dominated reaches, respectively.

$$\frac{\partial A}{\partial t} + \frac{\partial Q_w}{\partial x} = 0 \quad (13)$$

$$\frac{\partial Q_w}{\partial t} + \frac{\partial}{\partial x} \left(\alpha \frac{Q_w^2}{A} \right) + gA \frac{\partial h}{\partial x} + \frac{gQ_w |Q_w|}{C^2 RA} = 0 \quad (14)$$

$$(1 - \varepsilon) \frac{\partial Z_b}{\partial t} + \frac{\partial q_s}{\partial x} = 0 \quad (15)$$

in which A is the wet cross-sectional surface area (m^2), t is time (s), x is the longitudinal distance (m), α is the Boussinesq coefficient (-), R is the hydraulic radius (m), ε is the bed material porosity (40% for uniform sand), and Z_b is the bed level (m). The hydrodynamic model simulation is based on implicit time discretization, in which the stability of the solution does not depend on the Courant number, though this will influence the accuracy of the solution (Ali, 2014). On the contrary, the time step for the solution of the sediment continuity equation must satisfy the Courant number (σ).

$$\sigma = \alpha_c c \frac{\Delta_t}{\Delta_x} \leq 1 \quad (16)$$

where c is the bed disturbance celerity ($m s^{-1}$), Δ_t is the morphological time step (s), Δ_x is the grid size (m) and α_c is the stability factor to prevent non-linear instability (taken as 1.01, based on SOBEK-RE user manual).

The Lower reach has several bifurcations close to Lake Tana, but for SOBEK-RE model simulations we assume a single, 77 km long river (four reaches) from the dam site to Lake Tana.

3.5.2. Ribb River model construction

Model construction includes model setup, calibration and validation. For this study, the model was constructed and executed for three different dam operation scenarios (Section 3.2). Reach-averaged river bed slope, channel dimensions

(width and depth, assuming a rectangular channel), mean grain size, Chézy coefficient, and upstream and downstream boundary conditions were the required input parameters as described in Section 3.1 and listed in Table 1. The model development was based on the assumption of uniform bed material for each study reach. The general schematization of the SOBEK-RE model for the Ribb River is shown in Figure 3. All model simulations cover 1,500 years, as this period is assumed to be long enough to obtain a new morpho-dynamic equilibrium of the river reaches.

The measured average monthly river discharge and the average monthly dam releases (sum of irrigation demand, environmental flow, and spill-over discharge) were used as model input at the upper boundary to simulate the pre- and post-dam cases, respectively. A constant (time-averaged) Lake Tana water level was imposed at the downstream boundary for all simulation scenarios, even though this is variable and creates alternating local river bed erosion and deposition during the low and high stages, respectively. The long-term character of the study justifies using a constant level. The sediment transport rates of the Upper-I reach computed using Wong and Parker (2006)'s formula was used as the upstream boundary condition for the pre-dam case. For the post-dam cases, the sediment load at the upper boundary was set to zero, assuming that the dam blocks bed material movement to the downstream reaches. Discharge increment at the start of the Upper-II, Middle and Lower reaches due to the additional watershed area, and the water withdrawal for irrigation at the start of the Middle reach were introduced as lateral flows. Due to lack of data, the model neglects lateral sediment inputs by ephemeral tributaries, which may enter the river system during the rainy season. However, model sensitive to sediment supply was assessed by considering the release of 20% of the sediment transport capacity of the reaches to the downstream river from the dam as lateral sediment input (the released sediment volume depends on the dam operation scenarios).

The rock outcrops located at the end of Upper-I reach (around 1.2 km long) were introduced in the model as a non-erodible layer. Hence, in this river section no bed erosion occurs, but there may be some sediment deposition. The existence of this fixed river section controls the pre- and post-dam slope of the reaches. This section of the river cannot be taken into account by the ET, which is based on the assumption of an alluvial river without any geological constraints. In addition, assuming uniform bed material over

the depth may also yield uncertain results as there may be rock formation beneath the alluvial layers.

The diversion weir, located at the upstream boundary of the Middle reach, was included in the model as a structure. The weir temporarily affects the sediment movement causing aggradation and degradation at the upstream and downstream reaches, elongating the time that is necessary for achieving equilibrium (Jansen et al., 1979; Lanzoni et al., 2015).

The bed roughness, in terms of Chézy's coefficient, was selected as a calibration parameter to compute the water depths and compare with the measured values of the months from May to October 2007 at the Lower gauging station. Based on visual characteristics of the study reach, Chézy coefficient values ranging from $30 \text{ m}^{1/2} \text{ s}^{-1}$ to $40 \text{ m}^{1/2} \text{ s}^{-1}$ were considered. The runs were carried out assuming that the upstream effects of backwater and floodplain flow are negligible, which may occur in the Lower reach if the discharge is above bank full discharge ($110 \text{ m}^3 \text{ s}^{-1}$). The Root Mean Square Error (RMSE), Equation (17), which measures the difference between the observed values and the model outputs, was used to identify the best value of Chézy coefficient. RMSE value close to zero indicates a good fit.

$$\text{RMSE} = \sqrt{\frac{\sum_{i=1}^n (X_i - X_0)^2}{n}} \quad (17)$$

where X_i and X_0 are the measured and the model output (estimated) water levels and n is the number of samples. For validation, the calibrated model was run from May to October 2008. The computed water levels at the Lower gauging station were then compared to those measured, and RMSE was calculated.

The accuracy of the computed sediment transport capacity using a sediment transport formula may be limited due to the many uncertainties related to the physical characterization of the river reach and its hydraulic regime (Schmidt & Wilcock, 2008). Sensitivity analyses should thus be carried out to study the effects of varying the value of specific variables characterized by strong uncertainty (Hamby, 1994). In this study, a sensitivity analysis was carried out to analyse the effects of grain size on bed load in the Upper-I reach and on river bed degradation near the toe of the dam after 100 years for the range of D_m values from 6 to 8 mm. The obtained results were then compared with the results of the base-case scenario (Sc-II).

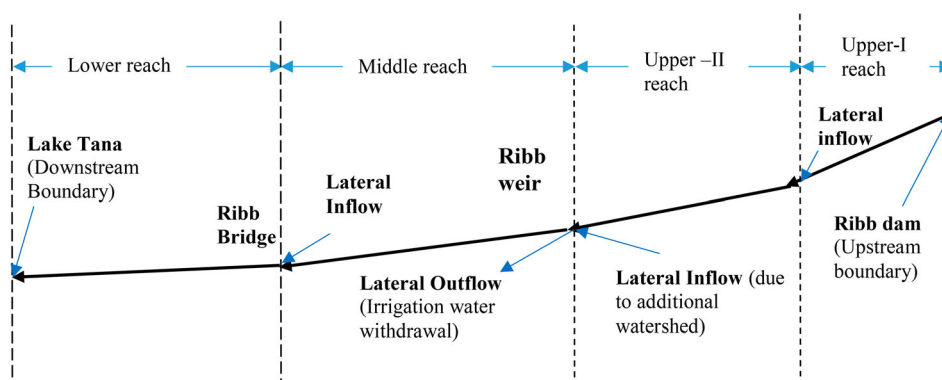


Figure 3. 1D model schematization with boundary conditions and location of hydraulic structures. Lateral inflow is the discharge due to additional watershed area, while the lateral outflow is the water withdrawal to the irrigation command areas by the diversion weir.

4. Results

4.1. Pre and post-dam river discharges

The average monthly excess discharge that is expected to spill-over from the reservoir, computed from the reservoir water balance (Equation 1), is shown in Table 3. On average, the reservoir is expected to be full at the end of July and the spill-over to continue until October. In all dam operation scenarios, the total yearly volume of water flow in the Upper-I and Upper-II reaches will not be affected by the dam, except for the first year to fill the reservoir.

The average pre- and post-dam monthly discharge hydrographs for the downstream river reaches are shown in Figure 4. The pre-dam hydrograph is directly related to the amount of rainfall and the watershed properties and shows one peak discharge period per year. After regulation, the Upper-I (Figure 4(a)) and Upper-II (Figure 4(b)) reaches will experience two peaks per year. The wet period peak is due to excess discharge from the reservoir, while the dry period peak is due to the maximum water release from the reservoir for irrigation. For the Sc-III dam operation the wet season peak in the Upper-I reach is shifted by one month (from August to September) and reverted back in the Upper-II reach. This is due to the additional discharge from the ungauged watershed. On average, the Sc-II dam

Table 3. Average monthly spill-over discharge for the three dam operation scenarios.

Scenarios	Average monthly spill-over discharge ($\text{m}^3 \text{s}^{-1}$)			
	November to July	August	September	October
Sc-I	0	32.4	15.4	1.4
Sc-II	0	27.2	15.4	1.1
Sc-III	0	9.8	15.4	0.1

operation reduces the unregulated wet period peak discharge by 34%, 25%, 21% and 21% for the Upper-I, Upper-II, Middle and Lower reaches, respectively.

At the start of the Middle reach, the major part of the discharge is diverted by the weir to the primary irrigation canal. It is found that the rate of diversion (ratio of yearly diverted to unregulated flow) will be 29%, 32%, and 43% for the Sc-I, Sc-II and Sc-III dam operations, respectively. The dry period river discharges in the Middle (Figure 4(c)) and Lower (Figure 4(d)) reaches will be rather small, since it will represent only the environmental flows.

4.2. Pre and post-dam reach-averaged sediment transport capacity

The monthly reach-averaged pre- and post-dam sediment transport capacity of the river is shown in Table 4. Here, the post-dam sediment transport capacity refers to the capacity of the river immediately after dam construction and filling of the reservoir, but before the occurrence of any morphological changes caused by dam construction. The sediment transport capacity will then gradually decrease due to reduced river bed slope and bed material coarsening. Even though the total yearly river discharge volume in the Upper-I and Upper-II reaches will not change, the sediment transport capacities will present an immediate reduction for all dam operation scenarios. This is due to the reduction of peak discharge values (Figure 4(a) and (b)). Overall, dam operation Sc-II shows a 53%, 62% and 42% yearly sediment transport capacity reduction in the Upper-I, Upper-II and Middle reaches, respectively, compared to the unregulated (pre-dam) yearly sediment transport capacity of the reaches. It should be noted that the yearly sediment transport

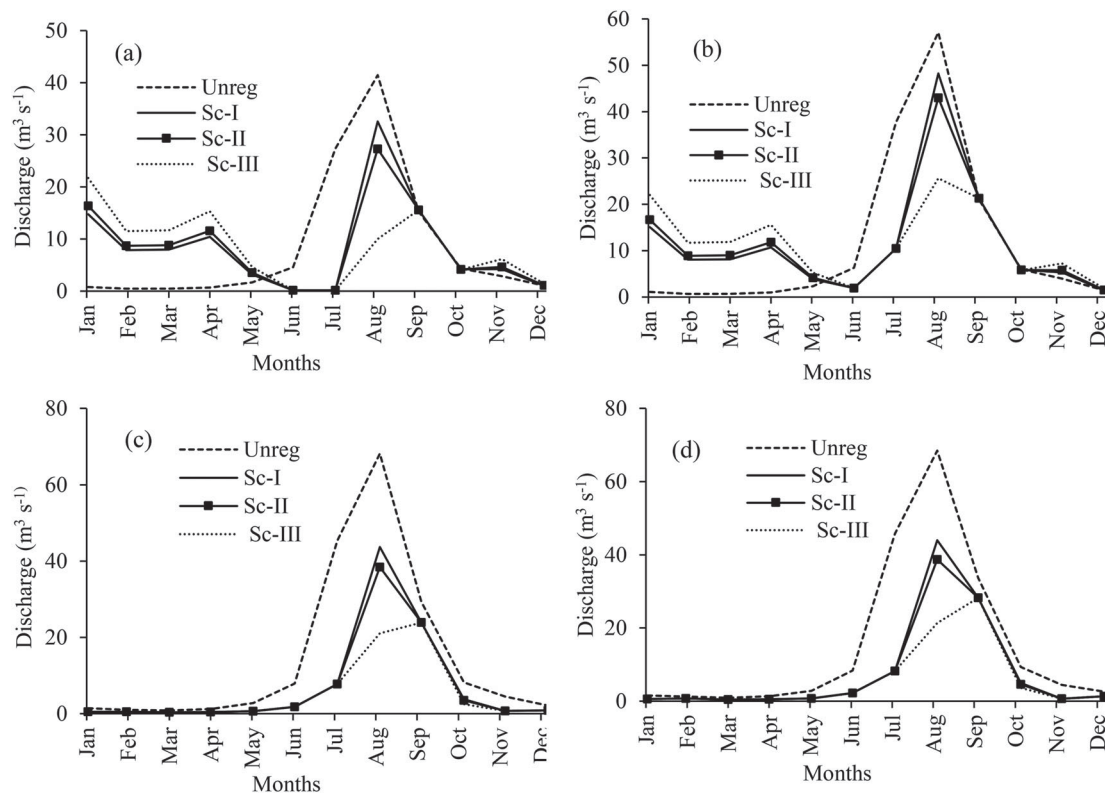


Figure 4. Average monthly discharge hydrograph for the four study reaches on the Ribb River for the unregulated (pre-dam) and the three regulated (post-dam) scenarios (Sc-I, Sc-II and Sc-III). (a) Upper-I, (b) Upper-II, (c) Middle and (d) Lower reaches.

Table 4. Pre- and post-dam reach-averaged yearly sediment transport capacity of Ribb River.

Reach	Pre-dam Q_s based on daily discharges Mulatu et al. (2018) ($1 \times 10^4 \text{ m}^3 \text{ year}^{-1}$)	Pre-dam Q_s based on monthly discharges ($1 \times 10^4 \text{ m}^3 \text{ year}^{-1}$)	Post-dam Q_s (immediately after dam construction) based on monthly discharges for different dam operation scenarios ($1 \times 10^4 \text{ m}^3 \text{ year}^{-1}$)		
			Sc-I	Sc-II	Sc-III
Upper-I	69.5	9.35	5.17	4.4	3.25
Upper-II	20	2.98	1.51	1.13	0.12
Middle	6.11	4.62	2.98	2.69	1.86

capacities computed based on monthly averaged discharges are substantially smaller than those obtained with the daily discharges, see Table 4.

The sensitivity of sediment transport capacity to the grain size was studied by changing D_m for Sc-II dam operation for the Upper-I reach. The analysis shows that, a reduction of D_m from 7 to 6 mm would result in a 32.7% increase of sediment transport capacity, while an increase of D_m from 7 to 8 mm would result in a 25.6% reduction. The difference is due to the non-linear relationship between sediment grain size and sediment transport capacity.

4.3. Results of the equilibrium theory

For the gravel-bed reaches, the theoretical equilibrium bed slopes attained by the river a long time after the start of the dam operation are computed with Equation (9). In the Upper-I reach, the three dam operation scenarios (Sc-I, II and III) result in longitudinal bed slopes of 0.088%, 0.105% and 0.132%, respectively, where the pre-dam slope being 0.30%. These slopes correspond to theoretical river bed degradations near the toe of the dam of 21.2, 19.5 and 16.8 m, respectively. Final-state theoretical river bed slopes of 0.053%, 0.06% and 0.1% are obtained for the Upper-II reach, where the pre-dam slope being 0.12%. For the upper reaches, the least-impacting scenario is Sc-III, corresponding to the largest water withdrawal for irrigation.

For the sand-bed Middle reach, the post-dam river bed slope is computed using Equation (12). In this case, the result is a flat river bed for all dam operation scenarios corresponding to a theoretical bed degradation of 10 m near the base of the weir. This indicates that the analytical method cannot differentiate the least-impacting dam operation scenarios in the sand-bed river reach if it is assumed that all incoming sediment is intercepted by the reservoir and for no sediment input from tributaries. Adopting the Engelund and Hansen (1967) formula implies assuming that the critical value of flow velocity for sediment motion is zero. This means that all dam operation scenarios with zero sediment input to the downstream river ultimately result in a theoretical flat river bed, since the approach did not consider other sediment sources, for instance ephemeral tributaries and bank erosion. Instead, using a sediment transport formula including a threshold for sediment motion, as the one used for the gravel-bed reaches (Wong & Parker, 2006), results in a different final bed slope for each discharge regime. However, for the assumed 20% sediment release to the downstream reaches (Section 3.5.2), the Middle reach may attain an equilibrium bed slope of 0.0017%, 0.0015% and 0.0010% for Sc-I, Sc-II and Sc-III dam operations, respectively.

4.4. Results of one dimensional morphodynamic model simulation

4.4.1. Model calibration and validation

The results of model calibration show that the measured and simulated water depth values agree quite well for a Chézy coefficient value of $35 \text{ m}^{1/2} \text{ s}^{-1}$ resulting in a RMSE value of 0.1 (Figure 5(a)). It is noticed that the model overestimates water levels at low-flows (Figure 5(b)). Note that the model overestimates water levels at low flows. Model validation also shows a good agreement between the measured and the simulated water depths (Figure 5(c)) with a corresponding RMSE of 0.10.

4.4.2. Model application on the Ribb River

The results of the long-term simulation of the calibrated and validated model show two patterns: degradation and aggradation, even though degradation dominates the river system. River bed degradation commences immediately after the start of dam operation at the base of the dam and at the base of the weir propagating in a downstream direction as time passes. At the end of the simulation period, the simulated river bed degradations at the base of the dam is 19, 17 and 12 m for Sc-I, Sc-II and Sc-III, respectively (Figure 6(a)). The simulated river bed degradation at the base of the dam is already 3.4, 2.9 and 2.2 m after 10 years from the start of dam operation for Sc-I, Sc-II and Sc-III, respectively. Bed degradation occurs at rates of 3.8, 3.3 and 2.3 cm year^{-1} in the first 5 years and continues at a rate of $\sim 0.1 \text{ cm year}^{-1}$ at the end of the computational period (Figure 6(a)). Two years after dam closure simulated bed degradation has extended to 3.2, 3 and 2.6 km from dam site for Sc-I, Sc-II and Sc-III, respectively, whereas it reaches the end of the Upper-I reach (10 km) after 100, 500 and 1,000 years, respectively (Figure 6(b)). At the end of the simulations, the reach-averaged river bed slope of the Upper-I reach is reduced to 0.106%, 0.125% and 0.155% for Sc-I, Sc-II and Sc-III, respectively.

In the Upper-II reach, the effects of the dam are felt only after the sediment leaving the Upper-I reach starts to decrease. In the meantime, the Upper-II reach is affected by the weir since sediment movement from upstream to downstream of the weir is zero for the first 40, 60 and 500 years for Sc-I, Sc-II and Sc-III, respectively, until the bed reaches the top of the weir (2.4 increase), Figure 7. Simulated bed degradation at the base of the weir is 2.1 m for Sc-I (Figure 7(a)) and 2.3 m for Sc-II (Figure 7(b)) in the first 50 and 80 years of model simulation, respectively. Thereafter, the transported sediment starts to pass over the weir temporally resulting in downstream bed aggradation, creating a new type of disturbance to the downstream reach. This bed aggradation process reduces the rate of morphological changes of the downstream reach. At the end of the simulation period, river

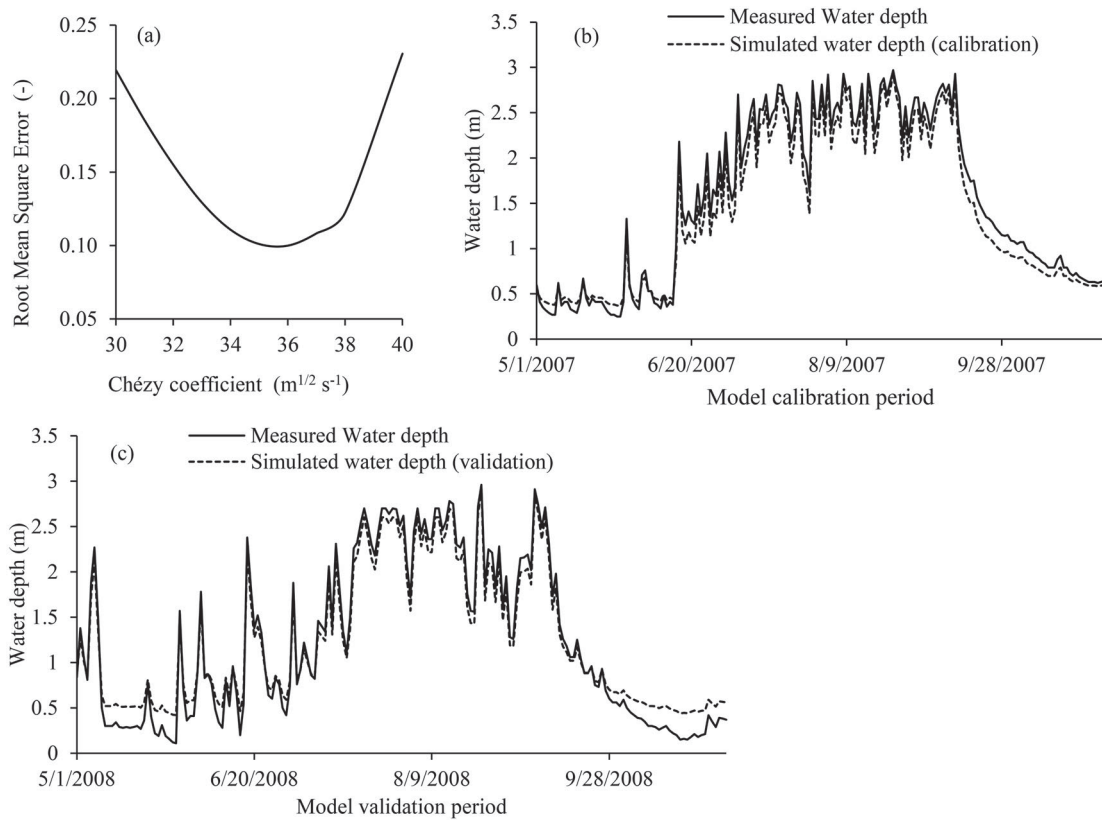


Figure 5. (a) Root Mean Square Error for different Chézy coefficient values. (b, c) Measured and simulated water depths at the Lower gauging station for the months of May to October 2007 (Calibration) and May to October 2008 (Validation), respectively.

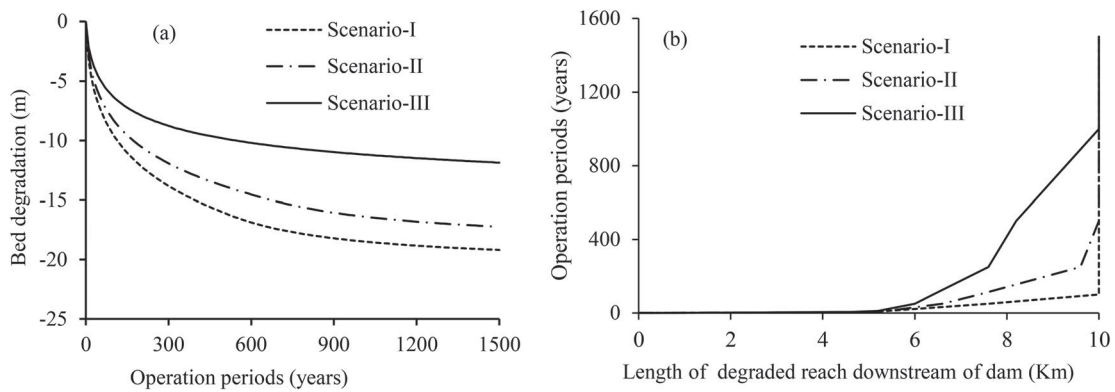


Figure 6. Results of the 1D morphodynamic model. (a) Ribb River bed degradation near the base of the dam for different dam operation scenarios over a 1,500 year period and (b) downward propagation of river bed degradation.

bed degradation near the base of the weir is 4.8 m (Figure 7 (a)), 5.0 m (Figure 7(b)), and 7.5 m (Figure 7(c)) for Sc-I, Sc-II and Sc-III, respectively. The maximum bed degradation at the base of the weir corresponds to the operation scenario with the highest rate of discharge diversion (Sc-III). Due to upstream river bed degradation, the reach-averaged bed slope of the Middle reach reduces to 0.029% for Sc-I and Sc-II and to 0.023% for Sc-III.

The results of the sensitivity analysis (Section 3.5.2) show that a decrease of D_m from 7 to 6 mm would increase the bed degradation at the dam base by 32.5%, whereas an increase of D_m from 7 to 8 mm would decrease the bed degradation by 25.2%. This clearly indicates that the model results are sensitive to the choice of mean sediment grain size.

4.5. Comparison of method results

Here, the results of the ET and 1D morphodynamic model are compared to assess the applicability of the analytical method to distinguish the impact of the different dam operation scenarios and to estimate the final slope of the river reaches. This would also allow to quickly calculate the value of bed degradation at the base of the dam and base of the weir. After 100 years of dam operation, the reach-averaged river bed slope of the Upper-I reach estimated with the 1D model is 51%, 45% and 36% steeper than the one estimated by the ET for the Sc-I, Sc-II and Sc-III, respectively. After 1,500 years, the bed slopes simulated by the 1D morphodynamic model are still 17%, 16% and 15% steeper than those predicted by the ET (Table 5). Similarly, the estimated river bed degradation at

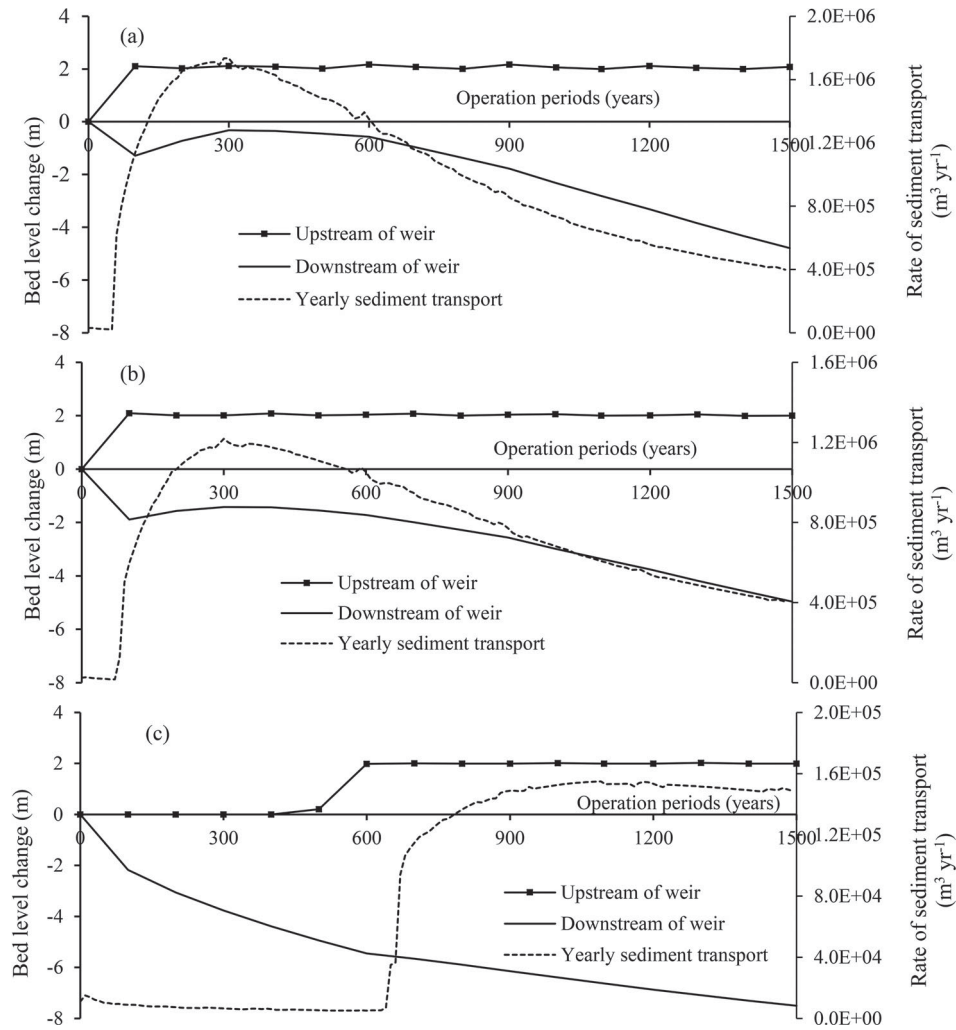


Figure 7. Simulated bed level changes immediately upstream and downstream of the Ribb weir, and simulated yearly sediment transport over the Ribb weir since start of the Ribb Dam operation for Sc-I (a), Sc-II (b) and Sc-III (c).

Table 5. Reach-averaged river bed slopes downstream of the Ribb Dam estimated using the Equilibrium Theory and the 1D model.

Reach	Current river bed slope (i_0), (%)	Simulation period (years)	Estimated river bed Slope (i_∞), (%)					
			1D model			Equilibrium Theory		
			Sc-I	Sc-II	Sc-III	Sc-I	Sc-II	Sc-III
Upper-I	0.3	100	0.178	0.191	0.206	0.088	0.105	0.132
		500	0.137	0.154	0.17			
		1,000	0.113	0.134	0.159			
		1,500	0.106	0.125	0.155			
Upper-II	0.12	100	0.12	0.12	0.132	0.053	0.060	0.100
		500	0.108	0.112	0.132			
		1,000	0.09	0.098	0.122			
		1,500	0.081	0.09	0.121			
Middle	0.04	100	0.036	0.033	0.033	0	0	0
		500	0.041	0.038	0.026			
		1,000	0.035	0.034	0.025			
		1,500	0.029	0.029	0.023			

the base of the dam by the ET exceed that obtained by the 1D model by 2.2, 2.5 and 4.8 m for the Sc-I, Sc-II and Sc-III, respectively. For the assumed 20% sediment release from the upper reaches the ET calculated a gentler slope for the Middle reach than the 1D model for all dam operation scenarios.

At the end of the 1D model simulation period, bed degradation at the base of the weir still occurs at rates ranging from 0.2 (Sc-III) to 0.46 cm year⁻¹ (Sc-I), indicating an on-going

morphological trend after 1,500 years. In general, the ET overestimates the morphological changes for both gravel-bed and sand-bed reaches compared to the 1D model for the considered period of model simulation, as shown in Table 5.

With the discussed limitations of the analytical and 1D morphodynamic models, we presented here the advantages gained and the easiness of the analytical approach compared with the 1D morphodynamic modelling (Table 6). The listed

Table 6. Comparison of analytical and 1D numerical models.

Description	Analytical approach (ET method)	1D modelling approach (SOBEK-RE)
Cost of input data	Can be applied for the reach-averaged river geometry.	Detail river channel cross-sectional surveying works or high resolution satellite images are required to extract river channel geometry.
Cost of modelling experience	Very simple to apply at field level to compare different sites and dam operation scenarios.	Modelling background and experience is required which incur costs to train experts.
Time for analysis	Results can be obtained within hours.	Results can be obtain after several days/weeks of modelling. Before simulation, substantial amount of time is required for model calibration and validation.

comparison items are not comprehensive, but assumed enough for discussion. From the comparison of results discussed above, we can say that the analytical models yields acceptable results for the comparison of different dam operation scenarios in the preliminary level of study for selecting the dam site.

5. Discussion

Geologically, the Upper Blue Nile basin is formed by a combination of tectonic-volcanic activities, and quaternary superficial processes (erosion and deposition) dominated by Oligocene-Miocene volcanic formations overlying by Quaternary alluvio-lacustrine deposit on the floodplain (Chorowicz et al., 1998). As described by Poppe et al. (2013) and Chorowicz et al. (1998), the basin shows gradual geological changes. This means that the long-term evolution of longitudinal river bed slope may not be affected by the geological setting and their dynamics (uplift, rifting and subsidence) and tectonic condition of the area. On the whole, the existence of disintegrated rock outcrops at some locations in the Upper-I and Upper-II reaches, sediment supply from ephemeral tributaries (Benda et al., 2004), bed material coarsening and armouring (Kondolf, 1997; Williams & Wolman, 1984) may limit the simulated depth of degradations and reach averaged slopes.

In gravel-dominated river reaches, post-dam sediment transport occurs only at discharges exceeding the limits for sediment motion (Gaeuman et al., 2005; Grant, 2012). Application of the Wong and Parker (2006) sediment transport capacity formula for the current river conditions (Section 4.2) shows that the bed material in the Upper-I and Upper-II reaches does not move if the discharge is less than 10 and 21.5 m³ s⁻¹, respectively. The reduced peak discharge during the wet season may not have the capacity to transport the largest sediment particles, thereby forming an armour bed surface (Grant, 2012; Kondolf, 1997), which could shorten the period to attain equilibrium. For the sand dominated reaches, the analysis shows that there may be some sediment movement for the entire range of flow releases until the river bed becomes completely flat for no sediment input from the upper reaches. However, the reaches may attain an equilibrium at a certain slope greater than the theoretical one as there may be sediment supplied during the rainy season from the ephemeral

tributaries. Generally, the morphological activities in the sand bed reaches dominate the morphological time scale of the Ribb River system. Similar results are also found for the Middle Yangtze River, China (Zhou et al., 2018). The overall reduction of flow in this reach may also create favourable conditions for the growth of vegetation in parts of the old channel which will reduce the channel width (Schmidt & Wilcock, 2008; Williams & Wolman, 1984).

The 1D model and the ET show that the dam operation scenario that yields the maximum dry- or wet-period peak flows (Sc-I) produces the maximum bed degradation downstream of the Ribb Dam, the minimum longitudinal bed slope in the upper reaches and the fastest downward propagation of bed degradation (Figure 6(b)). On the other hand, this scenario produces a relatively small morphological impact on the reach downstream of the weir, as some decades are required to replenish the degraded channel by the over-passed sediment (Figure 7(a)). It is important to note that a large portion of the total bed degradation at the dam base which requires remedial measures is obtained in the first 100 years, namely 58% for Sc-I and 56% for Sc-II and Sc-III dam operations.

The application of the ET, which assumes that the study reaches are fully alluvial, resulted in the assessments of the theoretical ultimate river bed slopes after the start of dam operation. These slopes are attained when no sediment deposition and no bed erosion take place in the considered reaches (new equilibrium). The results of this study show that the ET overestimates the morphological changes compared to the 1D model (after 1,500 years). Duró et al. (2016) found a good agreement between the slopes predicted by a 2D Delft3D morphological model and the ones derived with the ET by analysing the long-term morphological effects of channel width variations; though the ET tended to slightly overestimate the changes. The ET method can only be used to compare dam operation scenarios on the sand-dominated reaches if there is sediment supply from the upper reaches.

Li et al. (2014) suggested that a river system may be considered in equilibrium if the maximum bed level changes are less than 0.5 cm year⁻¹ at the upstream boundary. The analysis of the 1D model result shows that the bed level change rates are reduced to 0.5 cm year⁻¹ after 700 years for Sc-I and Sc-II and, after 400 years for Sc-III. De Vries (1975) derived the following formula for the assessment of the time scale of the morphological adaptation of entire river reaches (see also Jansen et al., 1979):

$$T = \frac{(1 - \varepsilon)3L^2Bi}{bQ_s} \quad (18)$$

in which T is the morphological adaptation time when the morphological change has attained 50% of the total.

De Vries (1975) estimated the 50% morphological change adaptation time of the Dutch Rhine River reach, assumed 200 km long, and found it to be 1,000 years. Similarly, Church (1995) analyzed the time scale for 50% morphological change adaptation of the Peace River, located in British Columbia and Alberta, to the operation of the WAC Bennett Dam, using the approach of De Vries (1975) and found it to be greater than 10,000 years for the upstream cobble dominated reach and 5,000 years for the sand dominated downstream reach. Di Silvio and Nones (2014) also found similar results, in which larger rivers may require hundreds and thousands of

years to attain a final equilibrium after disturbance. However, it was not possible to apply the same method to the entire Ribb River, from the dam site to the Lake Tana, because the weir and the water extraction for irrigation subdivide the river in two distinct parts, with different discharge regimes. Applying the method to the two parts of the river separately would strongly underestimate the adaptation time, considering that the morphological adaptation of the river reaches downstream of the weir are influenced by the morphological changes in the upper reaches, which affect the amounts of sediment bypassing the weir.

Both methods used in the study were based on simplifications that might affect their results, as, for instance, the use of reach-averaged channel geometries and granulometric characteristics. Furthermore, both methods did not include the sediment input from bank erosion and ephemeral tributaries. This introduces uncertainty into the computed results. Consequently, the river bed slopes obtained by both the ET and by 1D morphodynamic model should be interpreted as mere indications of the morphological adjustment, considering also that the river may never achieve equilibrium as the forcing and boundary conditions such as the river discharge, sediment yield, population density, land use, land cover, etc., fluctuate through time (Bolla Pittaluga et al., 2014). Nevertheless, both approaches used in this study allow discriminating the effects of different dam operation scenarios on gravel and sand-bed rivers. However, the application of the ET on sand-bed rivers is restricted to the cases in which some sediment is supplied from the upper reaches. Validation of both methods to determine if they indeed allow recognizing the least impacting scenario is difficult, considering that data showing the effects of different scenarios on the long-term river morphology are lacking.

6. Conclusions

This study addresses the applicability of physics-based analytical equations (Equilibrium Theory) compared to a 1D numerical model (SOBEK-RE) to determine the least-morphologically impactful dam operation scenario on the river reaches downstream of the under-construction Ribb River dam, which are dominated by gravel and sand. Three scenarios were evaluated: Sc-I, corresponding to a dam operation with a command area 10% smaller than the design command area; Sc-II, corresponding to a dam operation for the design command area; and Sc-III, corresponding to a dam operation with a command area 32.8% greater than the design command area.

Both methods show that Sc-I has the greatest morphological impact immediately downstream of the Ribb Dam, as it has the smallest reduction in peak discharge values (Figure 6(a)). The 1D model simulation showed a bed degradation at the dam base of 19 m after 1,500 years, whereas a bed degradation of 21.2 m was estimated by the ET. Bed degradation starts at the dam site and propagates downstream through time. Upstream of the weir the river bed gradually rises until it reaches the weir crest level. Immediately downstream of the weir, the river bed shows first degradation, then aggradation, starting when the upstream bed level has reached the crest, and then again degradation, starting when the sediment input from the reach Upper-II reduces to a value below the sediment transport capacity of the flow in the Middle reach. This type of alternating bed level changes

at the base of the weir slows down the morphological adaptation of the downstream sand-bed reaches considerably (Figure 7(b)).

The ET overestimates the morphological changes for both the gravel-bed and the sand-bed reaches compared to the 1D morphodynamic model for the specified period of model simulation, though both methods show relatively good agreement for the reach close to the dam (Upper-I). This is due to the over-simplification of the theory compared with the 1D model. In addition, the 1D model results show the existence of morphological activity in all the reaches even after 1,500 years for all dam operation scenarios (Section 4.4.2). Generally, the model comparison indicates that the ET can be used to roughly and quickly assess the morphological changes in river reaches downstream of a dam for feasibility studies, considering that the method tends to overestimate morphologic adjustment.

Like dams, the long-term operation of diversion weirs will affect the fractional movement of sediments (Jansen et al., 1979; Thoms & Walker, 1993). Application of the ET for the sand dominated river reaches downstream of the weir results in ultimate flat river bed, with a theoretical bed degradation of 10 m at the base of the weir for all dam operation scenarios for no additional sediment input either from the tributaries or released from the dam. However, the model can be used for detecting the least impacting dam operation scenario for sand dominated reaches if there is sediment supply from the upper reaches. The 1D model simulation for the weir downstream reaches show that the morphological equilibrium will not be attained before several centuries.

Acknowledgements

The authors acknowledge the Netherlands Fellowship Program (NFP) for the financial support of this research project and thank Dr. Kees Sloff (Assistant Professor at Delft University of Technology and Expert on fluvial river engineering and fluvial morphology at Deltares, Delft, The Netherlands) for his valuable support to setup SOBEK-RE model. We also highly acknowledged the anonymous reviewers and the editors for their constructive comments.

Disclosure statement

No potential conflict of interest was reported by the author(s).

Availability of data and materials

The datasets supporting the conclusions of this article are included within the article.

Consent for publication

All authors read the manuscript and agreed for the publication.

Ethics approval and consent to participate

The authors hereby declared that, this manuscript is not published or considered for publication elsewhere.

ORCID

Chalachew A. Mulatu  <http://orcid.org/0000-0003-2545-0705>
Michael M. Moges  <http://orcid.org/0000-0003-1920-6757>

References

- Ali, Y. S. A. (2014). *The impact of soil erosion in the upper Blue Nile on downstream reservoir sedimentation* [Doctoral dissertation]. IHE Delft, Institute for Water Education, Delft, The Netherlands. <http://resolver.tudelft.nl/uuid:8ac9e0a5-ec7e-4173-ada4-255a3b2ed908>
- Basson, G. (2004). Hydropower dams and fluvial morphological impacts —An African perspective. In *Proceedings of the united nations symposium on hydropower and sustainable development*, 27–29 October, Beijing, China.
- Benda, L., Andras, K., Miller, D., & Bigelow, P. (2004). Confluence effects in rivers: Interactions of basin scale, network geometry, and disturbance regimes. *Water Resources Research*, 40(5), Article 15. <https://doi.org/10.1029/2003WR002583>
- Berends, K. D., de Jongste, A., van der Mheen, M., & Ottevanger, W. (2015). *Implementation and verification of morphology in SOBEK 3* [Paper presented]. NCR-Days 2015, October 1–2, Nijmegen, Netherlands.
- Blom, A., Arkesteijn, L., Chavarrias, V., & Viparelli, E. (2017). The equilibrium alluvial river under variable flow and its channel-forming discharge. *Journal of Geophysical Research: Earth Surface*, 122(10), 1924–1948. <https://doi.org/10.1002/2017JF004213>
- Bolla Pittaluga, M., Luchi, R., & Seminara, G. (2014). On the equilibrium profile of river beds. *Journal of Geophysical Research: Earth Surface*, 119(2), 317–332. <https://doi.org/10.1002/2013JF002806>
- Brandt, S. A. (2000). Classification of geomorphological effects downstream of dams. *Catena*, 40(4), 375–401. [https://doi.org/10.1016/S0341-8162\(00\)00093-X](https://doi.org/10.1016/S0341-8162(00)00093-X)
- BRLi, & MCE. (2010). *Pump, drainage schemes at Megech: Environmental and Social Impact Assessment of the Ribb Irrigation and Drainage Project*.
- Brune, G. M. (1953). Trap efficiency of reservoirs. *Transactions, American Geophysical Union*, 34(3), 407–418. <https://doi.org/10.1029/TR034i003p00407>
- Chorowicz, J., Collet, B., Bonavia, F., Mohr, P., Parrot, J., & Korme, T. (1998). The Tana basin, Ethiopia: Intra-plateau uplift, rifting and subsidence. *Tectonophysics*, 295(3–4), 351–367. [https://doi.org/10.1016/S0040-1951\(98\)00128-0](https://doi.org/10.1016/S0040-1951(98)00128-0)
- Church, M. (1995). Geomorphic response to river flow regulation: Case studies and time-scales. *Regulated Rivers-Research and Management*, 11(1), 3–22. <https://doi.org/10.1002/rrr.3450110103>
- Curtis, K. E., Renshaw, C. E., Magilligan, F. J., & Dade, W. B. (2010). Temporal and spatial scales of geomorphic adjustments to reduced competency following flow regulation in bedload-dominated systems. *Geomorphology*, 118(1), 105–117. <https://doi.org/10.1016/j.geomorph.2009.12.012>
- De Vries, M. (1975). A morphological time scale for rivers. In *Proceedings of the 16th congress IAHR*, São Paulo, Brazil, 27 July–1 August, Vol. 2, 17–23.
- Di Silvio, G., & Nones, M. (2014). Morphodynamic reaction of a schematic river to sediment input changes: Analytical approaches. *Geomorphology*, 215, 74–82. <https://doi.org/10.1016/j.geomorph.2013.05.021>
- Duró, G., Crosato, A., & Tassi, P. (2016). Numerical study on river bar response to spatial variations of channel width. *Advances in Water Resources*, 93(A), 21–38. <https://doi.org/10.1016/j.advwatres.2015.10.003>
- Engelund, F., & Hansen, E. (1967). *A Monograph on sediment transport in alluvial streams*. Copenhagen, Denmark: Tech. Rep., Hydraul. Lab., Technical University of Denmark, p. 63.
- Exner, F. M. (1925). Über die wechselwirkung zwischen wasser und geschiebe in flüssen. *J34(2a)*, 165–204.
- Gaeuman, D., Schmidt, J. C., & Wilcock, P. R. (2005). Complex channel responses to changes in stream flow and sediment supply on the lower Duchesne river, Utah. *Geomorphology*, 64(3), 185–206. <https://doi.org/10.1016/j.geomorph.2004.06.007>
- Graf, W. (2006). Downstream hydrologic and geomorphic effects of large dams on American rivers. *Geomorphology*, 79(3), 336–360. <https://doi.org/10.1016/j.geomorph.2006.06.022>
- Grant, G. E. (2012). The geomorphic response of gravel bed rivers to dams: Perspectives and prospects. In *Gravel-bed rivers: Processes, tools, environments*, 165–181. <https://doi.org/10.1002/9781119952497.ch15>
- Grant, G. E., Schmidt, J. C., & Lewis, S. L. (2003). A geological framework for interpreting downstream effects of dams on rivers. *Water Science and Application*, 7, 209–225. <https://doi.org/10.1029/007WS13>
- Hamby, D. (1994). A review of techniques for parameter sensitivity analysis of environmental models. *Environmental Monitoring and Assessment*, 32(2), 135–154. <https://doi.org/10.1007/BF00547132>
- Holly, F. M. Jr., & Karim, M. F. (1986). Simulation of Missouri river bed degradation. *Journal of Hydraulic Engineering*, 112(6), 497–516. [https://doi.org/10.1061/\(ASCE\)0733-9429\(1986\)112:6\(497\)](https://doi.org/10.1061/(ASCE)0733-9429(1986)112:6(497))
- ICOLD. (1998). *World register of dams*. International Commission on Large Dams.
- Jansen, P. P., Van Bendegom, L., De Vries, M., & Zenen, A. (1979). *Principles of river engineering. The non-tidal alluvial river*. Delftse Uitgevers Maatschappij B.V.
- Khan, O., Mwelwa-Mutekenya, E., Crosato, A., & Zhou, Y. (2014). Effects of dam operation on downstream river morphology: The case of the Middle Zambezi river. *Proceedings of the Institution of Civil Engineers – Water Management*, 167(10), 585–600. <https://doi.org/10.1680/wama.13.00122>
- Kondolf, G. M. (1997). PROFILE: Hungry water: Effects of dams and gravel mining on river channels. *Environmental Management*, 7(4), 303–325.
- Kondolf, G. M., Gao, Y., Annandale, G. W., Morris, G. L., Jiang, E., Zhang, J., Cao, Y., Carling, P., Fu, K., Guo, Q., Hotchkiss, R., Peteuil, C., Sumi, T., Wang, H.-W., Wang, Z., Wei, Z., Wu, B., Wu, C., & Yang, C. T. (2014a). Sustainable sediment management in reservoirs and regulated rivers: Experiences from five continents. *Earth's Future*, 2(5), 256–280. <https://doi.org/10.1002/2013EF000184>
- Kondolf, G. M., Rubin, Z. K., & Minear, J. T. (2014b). Dams on the Mekong: Cumulative sediment starvation. *Water Resources Research*, 50(6), 5158–5169. <https://doi.org/10.1002/2013WR014651>
- Lanzoni, S., Luchi, R., & Pittaluga, M. B. (2015). Modeling the morphodynamic equilibrium of an intermediate reach of the Po river (Italy). *Advances in Water Resources*, 81, 95–102. <https://doi.org/10.1016/j.advwatres.2014.11.004>
- Li, S., Li, Y., Yuan, J., Zhang, W., Chai, Y., & Ren, J. (2018). The impacts of the three Gorges Dam upon dynamic adjustment mode alterations in the Jingjiang reach of the Yangtze river, China. *Geomorphology*, 318, 230–239. <https://doi.org/10.1016/j.geomorph.2018.06.020>
- Li, W., Wang, Z., de Vriend, H. J., & van Maren, D. S. (2014). Long-term effects of water diversions on the longitudinal flow and bed profiles. *Journal of Hydraulic Engineering*, 140(6), Article 04014021. [https://doi.org/10.1061/\(ASCE\)HY.1943-7900.0000856](https://doi.org/10.1061/(ASCE)HY.1943-7900.0000856)
- Meyer-Peter, E., Müller, R. (1948). Formulas for bed-Load transport. In *Proceedings of the international association for hydraulic research (IAHR) 2nd Meeting*, 7–9 June, Stockholm, Sweden.
- Mulatu, C. A., Crosato, A., Moges, M. M., Langendoen, E. J., & McClain, M. (2018). Morphodynamic trends of the Ribb river, Ethiopia, prior to dam construction. *Geosciences*, 8(7), Article 255. <https://doi.org/10.3390/geosciences8070255>
- Nones, M., Guerrero, M., & Ronco, P. (2014). Opportunities from low-resolution modelling of river morphology in remote parts of the world. *Earth Surface Dynamics*, 2(1), 9–19. <https://doi.org/10.5194/esurf-2-9-2014>
- Nones, M., Varrani, A., Franzioia, M., & Di Silvio, G. (2019). Assessing quasi-equilibrium fining and concavity of present rivers: A modelling approach. *Catena*, 181, Article 104073. <https://doi.org/10.1016/j.catena.2019.104073>
- Omer, A., Ali, Y., Roelvink, J., Dastgheib, A., Paron, P., & Crosato, A. (2015). Modelling of sedimentation processes inside Roseires reservoir (Sudan). *Earth Surface Dynamics*, 3(2), 223–238. <https://doi.org/10.5194/esurf-3-223-2015>
- Petts, G. E. (1979). Complex response of river channel morphology subsequent to reservoir construction. *Progress in Physical Geography: Earth and Environment*, 3(3), 329–362. <https://doi.org/10.1177/030913337900300302>
- Petts, G. E., & Gurnell, A. M. (2005). Dams and geomorphology: Research progress and future directions. *Geomorphology*, 71(1), 27–47. <https://doi.org/10.1016/j.geomorph.2004.02.015>
- Poppe, L., Frankl, A., Poesen, J., Admasu, T., Dessie, M., Adgo, E., Deckers, J., & Nyssen, J. (2013). Geomorphology of the Lake Tana basin, Ethiopia. *Journal of Maps*, 9(3), 431–437. <https://doi.org/10.1080/17445647.2013.801000>
- Sanyal, J. (2017). Predicting possible effects of dams on downstream river bed changes of a Himalayan river with morphodynamic modelling. *Quaternary International*, 453, 48–62. <https://doi.org/10.1016/j.quaint.2017.03.063>

- Schmidt, J. C., & Wilcock, P. R. (2008). Metrics for assessing the downstream effects of dams. *Water Resources Research*, 44(4). <https://doi.org/10.1029/2006WR005092>
- Setegn, S. G., Srinivasan, R., & Dargahi, B. (2008). Hydrological modeling in the Lake Tana Basin, Ethiopia using SWAT model. *The Open Hydrology Journal*, 2(2008), 49–62. <https://doi.org/10.2174/1874378100802010049>
- Shields, F. D. Jr., Simon, A., & Steffen, L. (2000). Reservoir effects on downstream river channel migration. *Environmental Conservation*, 27(1), 54–66. <https://doi.org/10.1017/S0376892900000072>
- SMEC. (2008). *Hydrological study of the Tana-Beles Sub-basin: Surface water investigation*. Snowy Mountains Engineering Corporation (SMEC) International Pty Ltd.
- Thoms, M., & Walker, K. (1993). Channel changes associated with two adjacent weirs on a regulated lowland alluvial river. *River Research and Applications*, 8(3), 271–284. <https://doi.org/10.1002/rrr.3450080306>
- Van der Zwet, J. (2012). *The creation of a reservoir in the White Volta river, Ghana: An analysis of the impact on river morphology* [M. Sc.]. TU Delftagris.fao.org
- Varrani, A., Nones, M., & Gupana, R. (2019). Long-term modelling of fluvial systems at the watershed scale: Examples from three case studies. *Journal of Hydrology*, 574, 1042–1052. <https://doi.org/10.1016/j.jhydrol.2019.05.012>
- Williams, G. P., & Wolman, M. G. (1984). *Downstream effects of dams on alluvial rivers*. U.S. Government Printing Office.
- Wong, M., & Parker, G. (2006). Reanalysis and correction of bed-load relation of Meyer-Peter and Müller using their own database. *Journal of Hydraulic Engineering*, 132(11), 1159–1168. [https://doi.org/10.1061/\(ASCE\)0733-9429\(2006\)132:11\(1159\)](https://doi.org/10.1061/(ASCE)0733-9429(2006)132:11(1159))
- WWDSE, & TAHAL. (2007). *Ribb Dam hydrological study (final report)*. Water Works Design and Supervision Enterprise (WWDSE) and TAHAL Consulting Engineers Ltd.
- Yang, S. L., Milliman, J. D., Li, P., & Xu, K. (2011). 50,000 dams later: Erosion of the Yangtze river and its delta. *Global and Planetary Change*, 75(1), 14–20. <https://doi.org/10.1016/j.gloplacha.2010.09.006>
- Zhou, M., Xia, J., Deng, S., Lu, J., & Lin, F. (2018). Channel adjustments in a gravel-sand bed reach owing to upstream damming. *Global and Planetary Change*, 170, 213–220. <https://doi.org/10.1016/j.gloplacha.2018.08.014>